Strong lensing and nonminimally coupled electromagnetism

Santiago E. P. Bergliaffa,[*] Edson Elias de Souza Filho[,†] and Rodrigo Maier[‡]

Departamento de Física Teórica, Instituto de Física, Universidade do Estado do Rio de Janeiro,
Rua São Francisco Xavier 524, Maracanã, CEP20550-900, Rio de Janeiro, Brazil

The lensing at large deflection angles caused by a Schwarzschild black hole for the case of a nonminimal coupling between gravitation and electromagnetism is examined. We show that photons follow an effective geometry, which displays an effective photon sphere. For the case in which the source, lens and observer are aligned, so that relativistic Einstein rings are formed, the dependence of the angular separation $\delta\theta$ between the first and second ring with the relevant coupling parameter is calculated. We argue that such a separation, which may be measured by telescopes that will be operative in the near future, may set an upper and a lower limit for the coupling parameter.

I. INTRODUCTION

The bending of light rays by a Schwarzschild black hole in the case in which the rays have an impact parameter close to $r = 3M$ (corresponding to the photon sphere of the black hole) is an example of lensing at large deflection angles.[1] Such a situation was studied first in [2],[2] reexamined in [4–7], and analyzed using a new lens equation for the deflection angle in [8]. It was shown in the latter reference that, considering the case where the observer, lens and source are aligned, an infinite sequence of relativistic Einstein rings is obtained. In the misaligned case, an infinite sequence of relativistic images (also called higher-order images) is produced on both sides of the optical axis, as well as the primary and the secondary images [8]. The relativistic images are very much demagnified, even in the case the source, the lens, and the observer are perfectly or highly aligned [9], although in the latter case the magnification is somewhat larger than the former. The analysis of lensing at large deflection angles was extended in [10], where the influence on the position of the relativistic images due to changes in the angular source position as well as the lens-source and lens-observer distances was studied. The strong lensing effect has been since then studied in a variety of systems, such as different types of black holes (see for instance [11–16], and wormholes [17]), among others.

It is important to stress that the above-mentioned results were obtained under the assumption of a minimal coupling between electromagnetism and gravity. However, more general couplings of the electromagnetic field to gravitation are possible, as reviewed in [18–20].[3] Among the multiple consequences of a nonminimal coupling (NMC), we can mention the following. The influence of such a coupling on the dispersion relation for waves was studied in [22]. Exact pp-wave solutions for gravity and electromagnetism in the NMC case were obtained in [23]. Black holes solutions for such a system were presented in [24], and reconsidered along with soliton solutions in [25], and in [26,27] with couplings of the type $f(R)F_{\mu\nu}F^{\mu\nu}$, while Einstein-Rosen bridges were obtained in [28]. A static nonminimally coupled test magnetic field around a Schwarzschild black hole was analyzed in [29]. In a cosmological setting, nonminimal couplings between EM and gravity were applied to Bianchi I models with a magnetic field in [30], while the influence of nonminimal couplings on the propagation of photons in the early universe was studied in [31].

Since, as discussed in [32], a possible NMC would not be probed by cosmological propagation of light or solar system tests of general relativity, we shall explore here the consequences of a NMC between gravitation and electromagnetism in the lensing at large deflection angles. In particular, we shall study the propagation of nonminimally coupled photons in the eikonal approximation in Schwarzschild's geometry. For those photons with impact parameter close to the effective photon sphere, we shall obtain the dependence of the angular separation of the relativistic Einstein rings (formed when the observer, the

---

[1]As opposed to lensing at small deflection angles (which may lead to multiple images) described in the weak gravitational field regime (sometimes called "strong lensing"), see for instance [1].
[2]See also [3].

[3]For the generalization of the nonminimal coupling to include an axion see [21].

lens, and the source are aligned) with the parameter corresponding to the NMC. In Sec. II, the theoretical formulation that leads to an effective geometry for the photons, due to the NMC between gravitation and electromagnetism, is presented. In Sec. III, we examine the effective potential, and show how the position of the effective photon sphere depends of the coupling parameter. In Sec. IV the dependence with the coupling parameter of the main quantities related to lensing at large deflection angles: the deflection angle α, the closest distance of approach R_0, and the angle θ of the image with respect to the optic axis is exhibited. Finally we present the plot of the angular separation of the first two rings as a function of the coupling. We draw our final remarks in Sec. V.

II. NONMINIMAL COUPLING AND THE EFFECTIVE GEOMETRY

Let $\mathcal{S}_p$ be the action for a photon in a gravitational field. The equation of motion for the electromagnetic field is then written as

$$\frac{\delta \mathcal{S}_p}{\delta A_\mu} = 0 \qquad (1)$$

where A_μ is the potential 4-vector connected to the Faraday tensor $F_{\mu\nu} = A_{\nu,\mu} - A_{\mu,\nu}$ and the commas denote usual partial differentiation. The minimally coupled part of $\mathcal{S}_p$ is given by the Maxwell Lagragian:

$$\mathcal{S}_0 = -\frac{1}{4} \int \sqrt{-g} F_{\mu\nu} F^{\mu\nu} d^4x. \qquad (2)$$

The nonminimally coupled sector is described by the action

$$\mathcal{S}_1 = \int \sqrt{-g} (\gamma_1 R F_{\mu\nu} F^{\mu\nu} + \gamma_2 R_{\mu\nu} F^\mu{}_\beta F^{\nu\beta} + \gamma_3 R_{\mu\nu\beta\sigma} F^{\mu\nu} F^{\beta\sigma}) d^4x, \qquad (3)$$

where γ_i ($i = 1, 2, 3$) are coupling coefficients, $R_{\mu\nu\beta\sigma}$ is the Riemann tensor, $R_{\mu\nu} \equiv R^\alpha{}_{\mu\alpha\nu}$, $R \equiv g^{\mu\nu} R_{\mu\nu}$ and ∇_μ is the covariant derivative built with the Christoffel symbols. Therefore, assuming that $\mathcal{S}_p = \mathcal{S}_0 + \mathcal{S}_1$, the equations of motion for the electromagnetic field can be rewritten as

$$\nabla_\mu F^{\mu\nu} + \frac{\delta \mathcal{S}_1}{\delta A_\nu} = 0. \qquad (4)$$

The corresponding equations of motion are[4]:

----

[4]These equations (with fixed values for the γs) can be obtained by considering QED vacuum polarization effects [33].

$$\nabla_\mu F^{\mu\nu} + 2\nabla_\mu [2\gamma_1 R F^{\mu\nu} + \gamma_2 (R^\mu{}_\beta F^{\beta\nu} - R^\nu{}_\beta F^{\beta\mu}) + 2\gamma_3 R^{\mu\nu}{}_{\beta\sigma} F^{\beta\sigma}] = 0. \qquad (5)$$

Restricting to vacuum spacetimes which satisfy Einstein's field equations $R_{\mu\nu} = 0$, equation (5) reads

$$\nabla_\mu F^{\mu\nu} + 4\gamma_3 \nabla_\mu (R^{\mu\nu}{}_{\beta\sigma} F^{\beta\sigma}) = 0. \qquad (6)$$

The electromagnetic tensor obeys also the Bianchi identity:

$$\nabla_\alpha F_{\mu\nu} + \nabla_\mu F_{\nu\alpha} + \nabla_\nu F_{\alpha\mu} = 0, \qquad (7)$$

To study the lensing of rays governed by Eqs. (6) and (7) in a Schwarzschild spacetime, we shall use the eikonal approximation, in which the test electromagnetic field is given by

$$F_{\mu\nu} = f_{\mu\nu} e^{i\theta}, \qquad (8)$$

where the phase θ is a very rapidly varying function (on scales much lower than the curvature scale, and much higher than the Compton wavelength of the electron) compared to the amplitude $f_{\mu\nu}$. By defining $k_\mu := \theta_{,\mu}$, Eq. (6) yields

$$k_\mu f^{\mu\nu} + 4\gamma_3 k_\mu R^{\mu\nu}{}_{\beta\sigma} f^{\beta\sigma} = 0. \qquad (9)$$

On the other hand, we obtain from the Bianchi identities (7),

$$k_\alpha f_{\mu\nu} + k_\mu f_{\nu\alpha} + k_\nu f_{\alpha\mu} = 0. \qquad (10)$$

Contracting Eq. (10) with k^α and using Eq. (7) we obtain

$$k^2 f_{\mu\nu} + 4\gamma_3 k_\alpha (k_\mu R^\alpha{}_{\nu\beta\sigma} - k_\nu R^\alpha{}_{\mu\beta\sigma}) f^{\beta\sigma} = 0. \qquad (11)$$

From the Schwarzschild metric given in standard coordinates $x^\alpha = (t, r, \theta, \phi)$,

$$ds^2 = \left(1 - \frac{2M}{r}\right) dt^2 - \left(1 - \frac{2M}{r}\right)^{-1} dr^2 - r^2 (d\theta^2 + \sin^2\theta d\phi^2), \qquad (12)$$

an orthonormal tetrad as the base of 1-forms

$$\Theta^A := e^A{}_\alpha dx^\alpha \qquad (13)$$

can be defined, where

$$e^A{}_\alpha \to \text{diag}\left(\sqrt{1 - \frac{2M}{r}}, 1/\sqrt{1 - \frac{2M}{r}}, r, r\sin\theta\right). \qquad (14)$$

Hence the line element can be written as

$$ds^2 = \eta_{AB} \Theta^A \Theta^B, \qquad (15)$$

where η_{AB} is the usual Minkowski metric of the tangent space. Let Q^{AB} and Ω^{AB} be two bivectors defined as

$$Q^{AB} = \sqrt{-g^{tt}g^{rr}}(e^A{}_t e^B{}_r - e^A{}_r e^B{}_t), \qquad (16)$$

$$\Omega^{AB} = \sqrt{g^{\theta\theta}g^{\phi\phi}}(e^A{}_\theta e^B{}_\phi - e^A{}_\phi e^B{}_\theta), \qquad (17)$$

so that the Riemann tensor can be written as

$$R^\alpha{}_{\nu\beta\sigma} = \frac{M}{r^3}[\delta^\alpha{}_\beta g_{\nu\sigma} - \delta^\alpha{}_\sigma g_{\nu\beta}$$
$$+ 3(Q^\alpha{}_\nu Q_{\beta\sigma} - Q^\alpha{}_\nu \Omega_{\beta\sigma})], \qquad (18)$$

where $Q^{\alpha\beta} \equiv Q^{AB} e_A{}^\alpha e_B{}^\beta$ and $\Omega^{\alpha\beta} \equiv W^{AB} e_A{}^\alpha e_B{}^\beta$, with $e^A{}_\alpha e_A{}^\beta \equiv \delta^\alpha{}_\beta$. Substituting Eq. (18) in Eq. (11) we obtain

$$\left(1 + \frac{8M\gamma_3}{r^3}\right)k^2 f_{\mu\nu} + \frac{12M\gamma_3}{r^3} k_\alpha[k_\mu(Q^\alpha{}_\nu Q_{\beta\sigma} - \Omega^\alpha{}_\nu \Omega_{\beta\sigma})$$
$$- k_\nu(Q^\alpha{}_\mu Q_{\beta\sigma} - \Omega^\alpha{}_\mu \Omega_{\beta\sigma})]f^{\beta\sigma} = 0. \qquad (19)$$

Defining the scalars

$$q := Q_{\alpha\beta}f^{\alpha\beta} \quad \text{and} \quad \omega := \Omega_{\alpha\beta}f^{\alpha\beta}, \qquad (20)$$

together with the vectors

$$l^\mu := k_\alpha Q^{\alpha\mu} \quad \text{and} \quad m^\mu := k_\alpha \Omega^{\alpha\mu}, \qquad (21)$$

Eq. (19) turns into

$$k^2 f_{\mu\nu} + \frac{\Delta}{2}[q(k_\mu l_\nu - k_\nu l_\mu) - \omega(k_\mu m_\nu - k_\nu m_\mu)] = 0, \qquad (22)$$

where

$$\Delta = \frac{24M\gamma_3}{r^3 + 8M\gamma_3}. \qquad (23)$$

By contracting Eq. (22) with $Q^{\mu\nu}$ we obtain

$$(k^2 + l^2 \Delta)q = 0, \qquad (24)$$

where $l^2 \equiv l_\mu l^\mu$. Since $q \neq 0$, the modified light cone follows from $k^2 + l^2\Delta = 0$ [33], or

$$(1 - \Delta)(k_t k^t + k_r k^r) + k_\theta k^\theta + k_\phi k^\phi = 0. \qquad (25)$$

The latter leads to the effective geometry $\tilde{g}_{\mu\nu}$ (see [34] for a review), in such a way that the line element for the light rays in the nonminimally coupled case is given by[5]

$$\overline{}$$

[5]A similar expression was obtained in [32].

$$d\tilde{s}^2 = \tilde{g}_{\mu\nu}dx^\mu dx^\nu = \left(1 - \frac{1}{R}\right)(1 - \Delta)dT^2$$
$$- \left(1 - \frac{1}{R}\right)^{-1}(1 - \Delta)dR^2 - R^2(d\theta^2 + \sin\theta d\phi^2), \qquad (26)$$

with

$$T = \frac{t}{2M}, \qquad R = \frac{r}{2M}, \qquad \Delta = \frac{3\Gamma_3}{R^3 + \Gamma_3}, \qquad (27)$$

and $\Gamma_3 \equiv \gamma_3/M^2$. Notice that the zero of $1 - \Delta$, given by $R_e = (2\Gamma_3)^{1/2}$ is such that $R_e \ll 1$, since we expect that $\Gamma_3 \ll 1$.

III. THE EFFECTIVE POTENTIAL

Let us consider a photon which follows a null geodesic in the effective metric defined by Eq. (26). The first integral of the equations of motion reads

$$f(R)\left(\frac{dT}{d\lambda}\right)^2 - \frac{1}{g(R)}\left(\frac{dR}{d\lambda}\right)^2 - R^2\left(\frac{d\theta}{d\lambda}\right)^2$$
$$- R^2\sin^2\theta\left(\frac{d\phi}{d\lambda}\right)^2 = 0, \qquad (28)$$

where λ is an affine parameter and

$$f(R) = \left(1 - \frac{1}{R}\right)(1 - \Delta), \qquad (29)$$

$$g(R) = \left(1 - \frac{1}{R}\right)(1 - \Delta)^{-1}. \qquad (30)$$

The symmetries of the background metric guarantee the existence of two constants of motion, namely E and $\mathcal{J}$, given by

$$E = f(R)\frac{dT}{d\lambda} \quad \text{and} \quad \mathcal{J} = R^2 \frac{d\phi}{d\lambda}. \qquad (31)$$

Therefore, the above first integral can be rewritten as

$$\frac{f(R)}{g(R)}\left(\frac{dR}{d\lambda}\right)^2 + V_{\text{eff}}(R) = E^2. \qquad (32)$$

where

$$V_{\text{eff}}(R) \equiv f(R)\frac{\mathcal{J}^2}{R^2} \qquad (33)$$

is the effective potential, the maximum of which defines the photon sphere R_p. Feeding Eq. (33) with Eq. (29), it is straightforward to see that the solutions of

FIG. 1. R_p as a function of Γ_3.

$$\left.\frac{dV_{\text{eff}}}{dR}\right|_{R_p} = 0 \qquad (34)$$

are given by

$$\Gamma_{3\pm} = \left[\frac{(12 - 11R_p) \pm 3\sqrt{24 + R_p(17R_p - 40)}}{4(2R_p - 3)}\right]R_p^3.$$

$$(35)$$

It follows that

$$\lim_{R_p \to 1}\Gamma_{3+} = -1 \quad \text{and} \quad \lim_{R_p \to 1}\Gamma_{3-} = \frac{1}{2}. \qquad (36)$$

We shall consider here only the "+" branch, since the "−" branch does not allow small values of Γ_3.

For $-1 < \Gamma_3 < 1/2$ the effective potential V_{eff} looks like one in the $\Gamma_3 = 0$ case. In particular, it exhibits only one global maximum R_{p+}, which is the effective photon sphere. In order to simplify our notation, instead of R_{p+} we will denote the global maximum just R_p in the following. The variation of R_p with Γ_3 is shown in Fig. 1.

IV. STRONG FIELD LENSING: MINIMAL VS NONMINIMAL COUPLING

We have seen in the previous section that the effective geometry given by Eq. (26) generates a modified light cone on which photons in the eikonal approximation propagate. Standard calculations (see for instance [35]) using the metric (26) instead of the Schwarzschild metric lead to the following expression for the deflection angle:

$$\alpha = 2 \int_{r_0}^{\infty} \frac{\sqrt{1 - \Delta}\,dr}{r\sqrt{\frac{r^2}{r_0^2}(1 - \frac{2M}{r_0})\frac{(1-\Delta_0)}{(1-\Delta)} - (1 - \frac{2M}{r})}} - \pi, \qquad (37)$$

FIG. 2.   Lens diagram. α is the Einstein deflection angle, β and θ are the angular position of the source and of its image with respect to the optic axis—defined by the line joining the observer O and the lens L. $\overline{LA}$ and $\overline{LB}$—which furnish the impact parameter $\mathcal{J}$—are perpendicular lines to $\overline{SD}$ and $\overline{OI}$, respectively. Finally, while D_{LS} is the lens-source distance, D_S and D_L are the distances of the source and the lens to the observer.

with impact parameter

$$\mathcal{J} = r_0 \left[\left(1 - \frac{2M}{r_0}\right)(1 - \Delta_0)\right]^{-\frac{1}{2}}, \qquad (38)$$

as shown in Fig. 2. Here r_0 is the closest distance of approach. For the purpose of computation, it is useful to use the rescaled coordinates introduced in Eq. (27). In this case, the deflection angle α can be written as

$$\alpha = 2 \int_{R_0}^{\infty} \frac{\sqrt{1 - \Delta}\,dR}{R\sqrt{\frac{R^2}{R_0^2}(1 - \frac{1}{R_0})\frac{(1-\Delta_0)}{(1-\Delta)} - (1 - \frac{1}{R})}} - \pi, \qquad (39)$$

and

$$\mathcal{J} = 2MR_0 \left[\left(1 - \frac{1}{R_0}\right)(1 - \Delta_0)\right]^{-\frac{1}{2}}. \qquad (40)$$

FIG. 3. The deflection angle α as a function of R_0 for $\Gamma_3 = 0$. The black curve is obtained in the first part of our numerical procedure (see text) where we use the integral in Eq. (39). The gray curves are the product of the second part of our numerical procedure, where we use the lens equation (45). The points of intersections between the black and gray curves furnish the angular deflections of the first and second relativistic Einstein rings.

All the formulas given here reduce to the minimally coupled case when $\Delta = 0.$[6]

In this paper we are going to consider a simple lens equation for asymptotically flat spacetimes originally introduced by K. S. Virbhadra and G. F. R. Ellis [8].[7] The lens diagram is depicted in Fig. 3. Let α be the Einstein deflection angle. If β and θ are the angles of the source and its image with respect to the optic axis—defined by the line joining the observer O and the lens L—the lens equation reads

$$\tan\beta = \tan\theta - \sigma, \qquad (41)$$

where it is assumed that both O and S are located far from the lens, in asymptotically flat regions, and

$$\sigma = \frac{D_{LS}}{D_S}[\tan\theta + \tan(\alpha - \theta)]. \qquad (42)$$

Furthermore, from the lens diagram we obtain that

$$\mathcal{J} = D_L \sin\theta. \qquad (43)$$

In order to better understand the gravitational lensing due to the nonminimal coupling, it is useful to bear in mind the

---

[6]In the weak field limit the integrand of (39) can be written as a power series of M/r and M/r_0. Following the standard calculation presented in [35], it can be shown that the correction due to Γ_3 is of the order of $(M^3/r^3, M^3/r_0^3)$. Hence, it is negligible in the weak field regime.

[7]The more general equation presented in [36,37] reduces to the one used here for the case in which the observer, lens and source are aligned.

results of the minimally coupled case [8]. It is well-known that for rays traveling through regions in which a spherically symmetric field gravitational field is weak an Einstein ring is formed when the source, lens and observer are aligned. Otherwise, a pair of images—usually called primary and secondary—of opposite parities is formed. Photons traveling close to the photon sphere (i.e., in the strong field regime), may go around the lens once, twice or many times. When the source, lens and observer are aligned, an infinite number of relativistic Einstein rings are formed due to the bending of light rays larger than 2π. For the case of misaligned components, an infinite sequence of relativistic images on both sides of the optic axis is obtained. We shall restrict here to the case in which the source, lens and observer are aligned in order to infer how the NMC affects the strong lensing. To compare our results with those in the literature, we assume that the lens is the supermassive black hole at the center of our Galaxy [8], so that the parameters are: $D_L = 8.5$ kpc, $M = 2.8 \times 10^6 \, M_\odot$, $D_S = 2D_{LS}$, where $M_\odot$ is the solar mass.

To evaluate the position of the relativistic Einstein rings we follow two different numerical procedures. The first one consists of the following steps:

(1.i) A finite number of pairs (Γ_3, R_p) is evaluated from Eq. (35), in the domain $-1 \le \Gamma_3 \le 0.5$;

(1.ii) For each value of Γ_3 a finite number of values of R_0, defined by $R_0(j) = R_p + j\epsilon$ is generated, where ϵ is a sufficiently small increment and j an integer;

(1.iii) Given $R_0(j)$ in (1.ii), we evaluate from Eq. (39) the corresponding values of α (for a fixed Γ_3).

The outcome of this first part is analogous to that of [38], and furnishes the plot of α as a function of R_0 for a fixed value of Γ_3 (cf. black curve in Fig. 4, built with $\Gamma_3 = 0$).

The second part of the procedure refers to the lens equation and is rather more involved:

(2.i) Equations (40) and (43) are evaluated at the distance of closest approach, namely the photon sphere, thus obtaining

$$D_L \sin\theta_p \equiv 2MR_p\left[\left(1 - \frac{1}{R_p}\right)(1 - \Delta_p)\right]^{-\frac{1}{2}}. \qquad (44)$$

Feeding (44) with each pair (Γ_3, R_p) from (1.i), the corresponding θ_p is evaluated;

(2.ii) For each numerical value of Γ_3 a finite number of values of θ_0, defined by $\theta_0(j) = \theta_p + j\tilde{\epsilon}$ is generated, where $\tilde{\epsilon}$ is a small increment and j an integer;

(2.iii) Inserting the $\theta_0(j)$ from (2.ii) in the lens equation

$$\tan\theta = \frac{D_{LS}}{D_S}[\tan\theta + \tan(\alpha - \theta)] \qquad (45)$$

the corresponding $\alpha(j)$ are obtained;
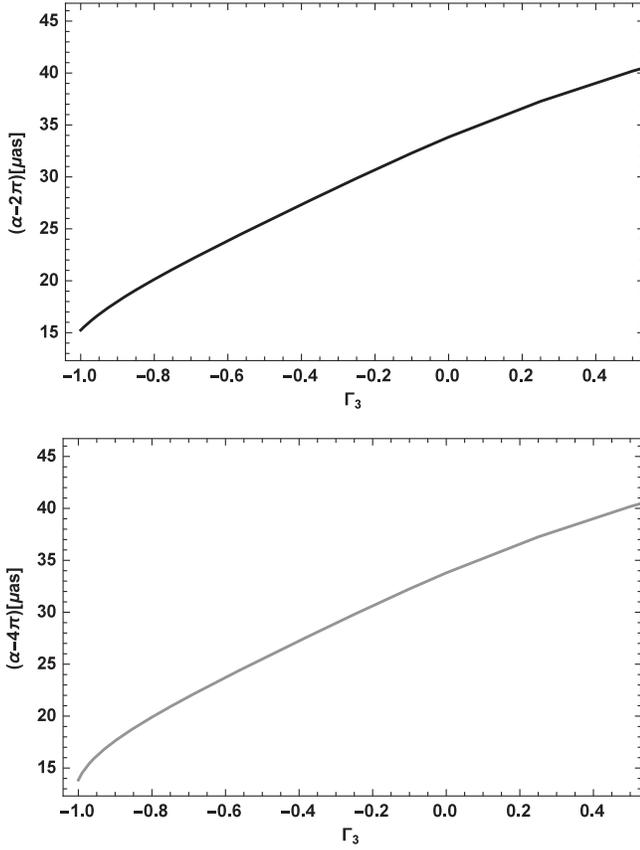
FIG. 4. Effective deflection angles as a function of the non-minimal coupling parameter of the first (upper panel) and second (lower panel) relativistic Einstein rings. The results for the minimally coupled case are recovered when $\Gamma_3 = 0$ [8].

(2.iv) Using Eqs. (40) and (43) so that

$$D_L \sin \theta_0 \equiv 2MR_0 \left[\left(1 - \frac{1}{R_0} \right) (1 - \Delta_0) \right]^{-\frac{1}{2}}, \quad (46)$$
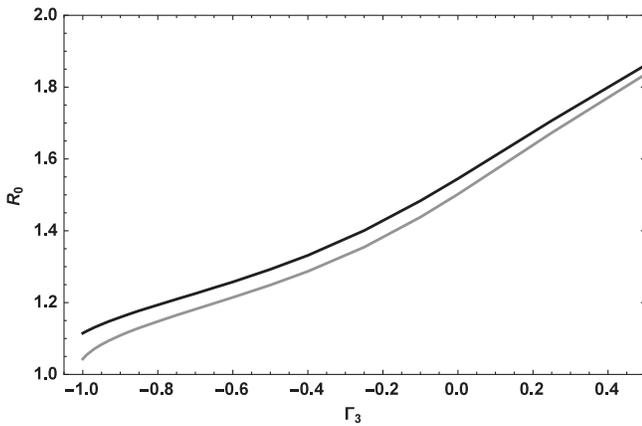
FIG. 5. The closest distance of approach R_0 as a function of Γ_3 for the first (black curve) and second (gray curve) relativistic Einstein rings.
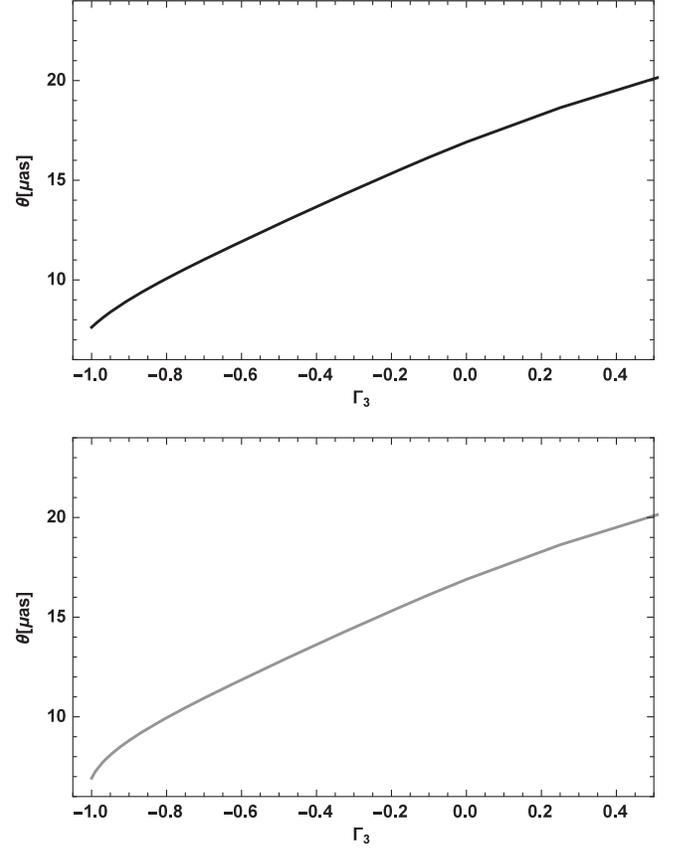
FIG. 6. The angular positions of the first (upper panel) and second (lower panel) relativistic Einstein rings as a function of Γ_3.

all the remaining $R_0(j)$ corresponding to $\theta_0(j)$ are evaluated.

As in the first part, this procedure allows to plot α as a function of R_0 for a fixed value of Γ_3 (see gray curves in Fig. 4). The points of intersection between the curve generated in the first part and the curves generated in the second part furnish the angular deflections of the first and second relativistic Einstein rings, given respectively by $2\pi + 33.80 \ \mu$as and $4\pi + 33.75 \ \mu$as [8].

We shall show next how the nonminimal coupling changes the values of α obtained for $\Gamma_3 = 0$. In Fig. 5 the effective deflection angle of the first (upper panel) and second (lower panel) relativistic Einstein rings are shown when the nonminimimal coupling is present. These plots show that, depending on the sign of Γ_3, the effective deflection angle can be smaller or larger than that of the minimally coupled case. For completeness, the distance of closest approach R_0 as a function of Γ_3 is shown in Fig 6 for both rings.

In Fig. 7 the angular position of the first (upper panel) and second (lower panel) relativistic Einstein rings as a function of Γ_3 is displayed. At this stage it is useful to distinguish such angles using a different notation: $\theta_{2\pi(4\pi)}$ denotes the angular position of the first (second) relativistic Einstein ring, and define the separation
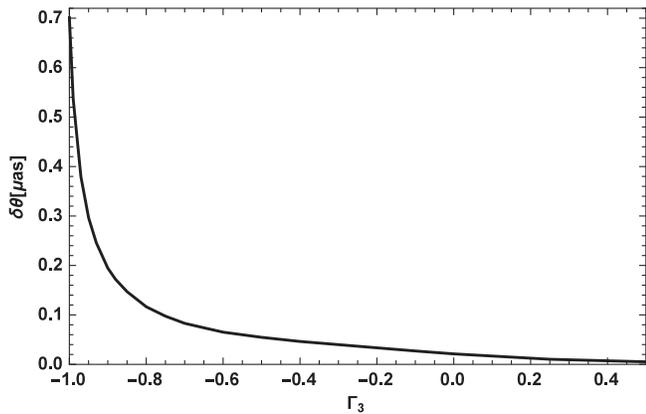
FIG. 7. The separation between the first and second relativistic Einstein rings as a function of Γ_3. This separation falls rapidly as Γ_3 increases, reaching the order of 5×10^{-3} μas for $\Gamma_3 = 0.5$.

$$\delta\theta = \theta_{2\pi} - \theta_{4\pi}. \qquad (47)$$

Figure 7 displays $\delta\theta$ as a function of Γ_3. It is worth noting that the result for the minimally coupled case (namely, $\delta\theta \approx 2 \times 10^{-2}$ μas [8]) is recovered in the limit $\Gamma_3 \to 0$.

V. FINAL REMARKS

We have examined strong deflection effects taking into account a nonminimal coupling between gravitation and electromagnetism. Assuming a Schwarzschild background, it was shown that the motion of photons in the eikonal limit is governed by an effective metric. The associated effective potential displays an effective photon sphere, the radius of which depends of Γ_3. We have analyzed here a particular configuration that displays strong field lensing effects in which the observer, the lens (taken as the supermassive black hole at the center of our Galaxy), and the source are aligned so that an infinite number of relativistic Einstein rings are formed. Using the lens equation introduced in [8], we evaluated in the strong field lensing regime the dependence with Γ_3 of the deflection angle α, the closest distance of approach R_0, and the angular position θ of the image with respect to the optical axis. Our results show that the angular separation $\delta\theta$ between the first and second Einstein rings can be as high as approx. 0.7 μas (for $\Gamma_3 = -1$), and falls rapidly as the coupling parameter Γ_3 increases, reaching the order of 10^{-3} μas for $\Gamma_3 = 0.5$.

It is worth noting that the highest resolution telescope available today (the *Event Horizon Telescope*) [39] has a resolution of the order of 25 μas, i.e., roughly 30 times larger than the separation between the first and second Einstein rings for $\Gamma_3 = -1$. Hence, it is not capable of detecting the maximum angular separation between two consecutive relativistic Einstein rings predicted by our results. If we assume that future observations yield a result that will not be very different from that of the minimally coupled case (which is of the order of 2×10^{-2} μas), at least a resolution of the order of 10^{-2} μas would be needed to set limits on Γ_3 using the results presented here. Such a resolution may be achieved by future instruments, in particular by the Millimetron Space Observatory [40] (which may have a resolution of approx. 50 narcsec at $\lambda = 0.345$ mm.). We should also point out that although the magnification for higher-order images is very small in the vacuum case, it becomes significantly larger in the presence of plasma [7,41]. Another important point is that a measure of $\delta\theta$ with its corresponding error would permit to set both an upper and a lower limit for Γ_3. This would an improvement with respect to the current situation, in which only upper limits are available [42].

The results presented here, based on the aligned configuration, show that it may be feasible in the future to use the separation of the relativistic rings to set limits on Γ_3.[8] The theoretical estimates presented here may improve if other configurations for the source-lens-observer system are studied. In particular, values different from $1/2$ for the ratio D_{LS}/D_S could be considered, as well as misaligned configurations. It would also be of interest to study how variations in the angular position of the source (together with changes in the lens-source distance) would furnish modifications—due to the nonminimal coupling—in the angular separations between any two relativistic images. Finally, the analysis should be extended to the more realistic case of a Kerr black hole In fact, as discussed in [44], precise measurements of the photon ring and even its subrings in this case are feasible using interferometry. We shall examine these points in future work.

---

[8]After this work was submitted for publication, we learned that some of the results presented here were obtained in [43] using a different method, with no reference to observational prospects.

[1] M. Bartelmann, Classical Quantum Gravity **27**, 233001 (2010).
[2] C. Darwin, Proc. R. Soc. A **249**, 180 (1959).
[3] R. d'Escourt Atkinson, Astron. J. **70**, 517 (1965).
[4] V. Perlick, Living Rev. Relativity **7**, 9 (2004).
[5] V. Perlick, in *Proceedings of the MG11 Meeting on General Relativity, Berlin, Germany, 2006*, edited by H. Kleinert, R. T. Jantzen, and R. Ruffini (World Scientific, Singapore, 2008), pp. 680699.
[6] V. Bozza, Gen. Relativ. Gravit. **42**, 2269 (2010).

[7] G. S. Bisnovatyi-Kogan and O. Y. Tsupko, Universe **3**, 57 (2017).

[8] K. S. Virbhadra and G. F. R. Ellis, Phys. Rev. D **62**, 084003 (2000).

[9] G. S. Bisnovatyi-Kogan and O. Yu. Tsupko, Astrophys. **51**, 99 (2008).

[10] K. S. Virbhadra, Phys. Rev. D **79**, 083004 (2009).

[11] L. Amarilla and E. F. Eiroa, Phys. Rev. D **85**, 064019 (2012).

[12] S.-W. Wei, Y.-X. Liu, C.-E. Fu, and K. Yang, J. Cosmol. Astropart. Phys. 12 (2012) 053.

[13] S.-W. Wei and Y.-X. Liu, J. Cosmol. Astropart. Phys. 13 (2013) 063.

[14] U. Papnoi, F. Atamurotov, S. G. Ghosh, and B. Ahmedov, Phys. Rev. D **90**, 024073 (2014).

[15] E. F. Eiroa, G. E. Romero, and D. F. Torres, Phys. Rev. D **66**, 024010 (2002).

[16] S. Chakraborty and S. SenGupta, J. Cosmol. Astropart. Phys. 07 (2017) 045.

[17] N. Tsukamoto, T. Harada, and K. Yajima, Phys. Rev. D **86**, 104062 (2012).

[18] H. F. M. Goenner, Found. Phys. **14**, 865 (1984).

[19] F. W. Hehl and Y. N. Obukhov, Lect. Notes Phys. **562**, 479 (2001).

[20] A. B. Balakin and J. P. S. Lemos, Classical Quantum Gravity **22**, 1867 (2005).

[21] A. B. Balakin and W.-T. Ni, Classical Quantum Gravity **27**, 055003 (2010).

[22] A. B. Balakin and A. E. Zayats, Classical Quantum Gravity **35**, 065006 (2018).

[23] T. Dereli and O. Sert, Phys. Rev. D **83**, 065005 (2011).

[24] F. Muller-Hoissen and R. Sippel, Classical Quantum Gravity **5**, 1473 (1988).

[25] A. B. Balakin, V. V. Bochkarev, and J. P. S. Lemos, Phys. Rev. D **77**, 084013 (2008).

[26] T. Dereli and O. Sert, Eur. Phys. J. C **71**, 1589 (2011).

[27] T. Dereli and O. Sert, Mod. Phys. Lett. A **26**, 1487 (2011).

[28] A. B. Balakin, J. P. S. Lemos, and A. E. Zayats, Phys. Rev. D **81**, 084015 (2010).

[29] P. Pavlović and M. Sossich, Phys. Rev. D **99**, 024011 (2019).

[30] A. B. Balakin and W. Zimdahl, Phys. Rev. D **71**, 124014 (2005).

[31] A. B. Balakin, V. V. Bochkarev, and J. P. S. Lemos, Phys. Rev. D **85**, 064015 (2012).

[32] Y.-Z. Chu, D. M. Jacobs, Y. Ng, and G. D. Starkman, Phys. Rev. D **82**, 064022 (2010).

[33] I. T. Drummond and S. J. Hathrell, Phys. Rev. D **22**, 343 (1980).

[34] C. Barceló, S. Liberati, and M. Visser, Living Rev. Relativity **8**, 12 (2005).

[35] S. Weinberg, *Gravitation and Cosmology: Principles and Applications of the General Theory of Relativity* (John Wiley & Sons, USA, 1972).

[36] V. Bozza, Phys. Rev. D **78**, 103005 (2008).

[37] A. B. Aazami, C. R. Keeton, and A. O. Petters, J. Math. Phys. (N.Y.) **52**, 092502 (2011).

[38] V. Bozza, Phys. Rev. D **66**, 103001 (2002).

[39] K. Akiyama *et al.*, Astrophys. J. **875**, L1 (2019).

[40] N. S. Kardashev *et al.*, Phys. Usp. **57**, 1199 (2014).

[41] O. Yu. Tsupko and G. S. Bisnovatyi-Kogan, Phys. Rev. D **87**, 124009 (2013).

[42] A. R. Prasanna and S. Mohanty, Classical Quantum Gravity **20**, 3023 (2003).

[43] S. Chen and J. Jing, J. Cosmol. Astropart. Phys. 10 (2015) 002.

[44] M. D. Johnson, A. Lupsasca, A. Strominger, G. N. Wong, S. Hadar, D. Kapec, R. Narayan, A. Chael, C. F. Gammie, P. Galison, D. C. M. Palumbo, S. S. Doeleman, L. Blackburn, M. Wielgus, D. W. Pesce, J. R. Farah, and J. M. Moran, Sci. Adv. **6**, eaaz1310 (2020).